



# Partitioning of polymers into pores with surface interactions at dilute solution limit

Yongmei Wang\*, Derek Howard, Yingchuan Gong

*Department of Chemistry, North Carolina Agricultural and Technical State University, Greensboro, NC 27411, USA*

Received 12 June 2003; received in revised form 8 November 2003; accepted 10 November 2003

## Abstract

The partitioning of a single polymer chain into a slit in a good solvent with different surface interactions is examined through Monte Carlo simulations from subcritical regime to adsorptive regime. The chain conformation in the subcritical regime is not perturbed by the surface interactions significantly. In the adsorptive regime, the conformation of the chain is strongly perturbed by the surface interactions. The confinement free energy in the two regimes maybe written in a uniform formula,  $\beta\Delta\mu_{\text{conf}} \sim c_1N(a/D)^x\varepsilon_w + c_2N(a/D)^{1/\nu}$  with  $x \sim 2.0$  or larger in the subcritical regime and  $\sim 1.0$  in the adsorptive regime, where  $\nu$  is the Flory exponent,  $D$  is the slit width,  $N$  is the chain length,  $a$  is the monomer size, and  $\varepsilon_w$  is the surface interaction energy between the polymer beads and the slit. This formula is valid for a long chain in the narrow slit in the subcritical regime or when the adsorption layer  $h > D$  in the adsorptive regime. A critical behavior occurs when  $\varepsilon_w$  is at the critical adsorption point and  $x = 1/\nu$ , then  $\Delta\mu_{\text{conf}}$  will have little dependence on  $N$  or  $D$ . Higher order terms that are neglected in the above equation, however, may be present that could lead to a weak dependence of  $K$  on  $N$  and  $D$  even in the critical adsorption point.

© 2003 Elsevier Ltd. All rights reserved.

*Keywords:* Monte Carlo simulation; Polymer partitioning; Adsorptive slit

## 1. Introduction

The partitioning of polymers into pores is an old subject and is important to chromatography separations of polymers such as gel-permeation chromatography (GPC) [1–10]. It has received extensive studies over the years [11–20]. Casassa developed a theoretical model for an ideal Gaussian chain confined in a slit and derived an analytical expression for the partitioning coefficient [1,2]. The theoretical result obtained has served as an important guide for experiments [10], though the ideal Gaussian chain is not a suitable model for real polymers. De Gennes has provided a scaling theory that accounts for the partitioning of both real polymer chains and ideal Gaussian chains into narrow pores [7]. Computer simulations have confirmed the predictions from the scaling theory [18]. The surfaces of the pore in these previous studies are assumed to be purely repulsive. Polymer chains are repelled from the surfaces. There was little interest to

consider pores with adsorptive surfaces because in most of the chromatography applications it is not desirable to have polymer adsorptions in the columns.

In recent years, new chromatography methods are being developed to separate complex polymer systems such as polymer blends, block copolymers and polymers with different stereo-regularity [21–26]. In these chromatography methods, attractive interactions of polymers with the pore surfaces are utilized. Liquid chromatography at critical adsorption point (LCCAC) is an example that makes use of the compensation of the enthalpic interaction with entropic interaction such that polymer chains are eluted independent of their molecular weights [22–24]. LCCAC coupled with regular GPC has found great use in separating block copolymers with different block compositions. These new chromatography methods, therefore, lead to new interests in studying the partitioning of polymers into pores with adsorptive surfaces.

Polymer adsorption on a solid surface is also an old subject and has received extensive studies [27–35]. The existence of trains, loops and tails in the adsorbed polymers and the thickness of the adsorbed layers have been well studied [34]. Polymers confined in a pore with adsorptive

\* Corresponding author. Present address: Department of Chemistry, University of Memphis, Memphis, TN 38152, USA. Tel.: +1-901-678-2629; fax: +1-901-678-3447.

*E-mail address:* [ywang@memphis.edu](mailto:ywang@memphis.edu) (Y. Wang).

surfaces, therefore, combine the two effects and have some interesting phenomenon. There are up to now few studies of chains in adsorptive pores [36–40]. Gorbunov and Skvortsov extended the theoretical model by Casassa to slits with adsorptive surfaces and examined many properties of the confined chains [36]. The results, however, are only applicable to ideal Gaussian chain. Milchev and Binder have performed computer simulations of a chain confined in a slit and a square pore with adsorptive surfaces [37–39]. They have examined the density profiles in the slit, radius of gyration of the chains and the mobility of the chain in the slit. However, they have not studied the equilibrium between the bulk solution and the pore. Cifra and Bleha systematically examined the influence of a number of factors including the surface interaction on polymer partitioning [40]. However, the range of surface interaction examined was somewhat limited to weak interactions.

Previously, we have studied the polymer partitioning into a slit near the critical adsorption point [41]. There we focused on the exact location of the critical point at which the enthalpic attraction and the entropic exclusion of the chain in the pore cancel with each other such that the partition coefficient of the chain in the pore may be one ( $K = 1$ ). We identified that this critical point exists for a random walk chain, and it corresponds to the critical adsorption point of a random walk chain above a surface. At the critical adsorption point, the partition coefficient of a random walk chain into a slit is exactly one ( $K = 1$ ), and is independent of the molecular weight of the chain. However, for a self-avoiding walk chain, one cannot find such a point at which  $K = 1$  and  $K$  is independent of the molecular weight of the chain at the same time. The cancellation between the entropic exclusion, and the enthalpic attraction does not occur at the same point for a self-avoiding walk chain. The closest to the ‘critical behavior’ is at the critical adsorption point of a self-avoiding walk chain above a solid surface. At this critical adsorption point, the partition coefficient is slightly above one ( $K^{\text{cr}}$  observed ranging from 1.05 to 1.6) and it has a very weak dependence on the molecular weight of the chain.

In the previous paper, the interaction between polymer/wall considered is very close to the critical adsorption point (the ‘critical regime’). In this paper, we extend our study into a wide range of surface interaction, from below the critical adsorption point (the ‘subcritical regime’) to above the critical adsorption point (the ‘adsorptive regime’), but we restrict this study to dilute solution limit and consider only the partitioning of a single polymer chain. The partition coefficients will have different dependence on the chain length  $N$ , slit width  $D$ , and the surface interaction  $\varepsilon_w$  in different regimes. Is there a universal function that can describe the dependence of  $K$  on  $\varepsilon_w$ ,  $N$  and  $D$  in each regime? What is the dominant term that determines the  $K$  in each regime? These are the questions that we would like to answer. One has to bear in mind that we probably cannot find a relationship that describes the data in the whole range

since the dependence of  $K$  on these parameters will change from one limit (non-adsorptive regime) to the other limit (critical or adsorptive regime). The best, we can find is the dominant terms in each regime and the interpolation between different regimes.

## 2. Simulation method

The slit is modeled by a simple cubic lattice with dimensions of  $250a \times 250a \times (D + 1)a$  along the  $x$ ,  $y$  and  $z$  directions. There are two solid walls located at  $z = a$  and  $z = (D + 1)a$  layers extending in the  $x$  and  $y$  directions. Polymer beads cannot occupy sites on the wall.  $D$  is the slit width, which is the distance between the two walls. A single polymer chain consisting of  $N$  beads is placed initially on the lattice and the reptation move with the metropolis rule is used to equilibrate the chain in the slit. The equilibration of the chain is monitored by monitoring the orientation correlation of the end-to-end vector of the chain. We found reptation move is sufficient to equilibrate a single chain in the pore in our study. The chain is a self-avoiding walk. There are no interactions between polymer beads except the excluded volume interaction, so the polymer chain is in an athermal solvent. The pore wall and polymer beads interaction is characterized by a nearest neighbor reduced interaction  $\varepsilon_w$  whenever a polymer bead is in direct contact with the sites on the wall. After an initial equilibration, 5000–10,000 snapshots of the chain, separated by  $\sim N^2$  steps, are collected and analyzed. We obtained the chemical potential of the chains in the slit, the density profiles across the slit, the radius of gyration of the chain in the  $xy$  and  $z$  components and the orientation of the chain inside the slit.

The partition coefficients for a single chain in the pore are obtained by comparing the chemical potential of a single chain in the bulk  $\mu_{\text{bulk}}$  and in the confined slit  $\mu_{\text{conf}}$  using the chain insertion method. The details of chain insertion method are given before [41,42]. The partition coefficient  $K$  for the chain at infinite dilute is given by  $-\ln K = \beta\Delta\mu_{\text{conf}} = \beta(\mu_{\text{conf}} - \mu_{\text{bulk}})$ .

## 3. Results and discussion

Fig. 1 presents the plot of  $\beta\Delta\mu_{\text{conf}}$  vs.  $2R_{g0}/D$  for a single chain with different chain lengths  $N = 25, 50, 100$  and  $200$ , partitioning into a slit of width  $D = 6$  at different surface interactions  $\varepsilon_w$ .  $R_{g0}$  is the radius of the gyration of the chain in the unconfined solution. The ratio  $2R_{g0}/D$  is the confinement strength. The longer the chain and the smaller the slit width, the stronger the confinement strength is. In Fig. 1, the slit width  $D$  is fixed, the variation of the confinement strength is only due to the change in the chain length. The critical adsorption point in our simulation model has been determined earlier [41] and was found to be

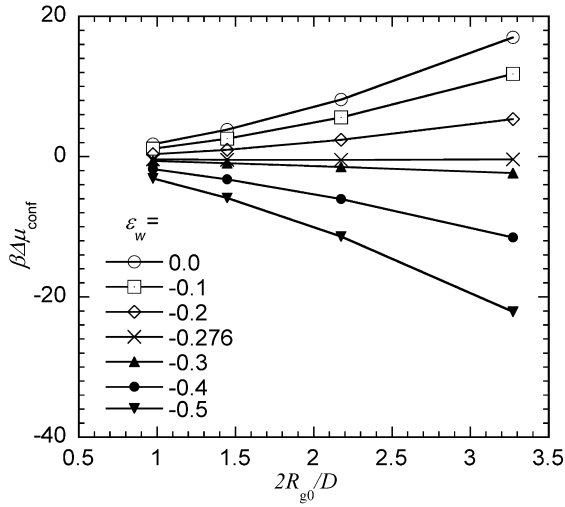


Fig. 1. The plot of confinement free energy  $\beta\Delta\mu_{\text{conf}}$  vs. the confinement strength  $2R_{g0}/D$  for a single chain with chain length  $N = 25, 50, 100,$  and  $200$  partitioning into a slit of width  $D = 6$  at different surface/wall interaction energies  $\varepsilon_w$ .

$\varepsilon_w^{\text{cr}} = -0.276$ . The critical adsorption point divides the data in Fig. 1 to two different regimes, the subcritical regime ( $|\varepsilon_w| < 0.276$ ) and the adsorptive regime ( $|\varepsilon_w| > 0.276$ ). The variation of the confinement free energy on the confinement strength is distinctly different in the two regimes. In the subcritical regime,  $\beta\Delta\mu_{\text{conf}}$  increases with the confinement strength. Longer polymer chains experience a larger confinement free energy cost in a slit than the shorter polymer chains. In the adsorptive regime, it is the reverse. Longer polymer chains are more strongly adsorbed in the slit than the shorter polymer chains. Below we will discuss the properties of the chain in the slit for the two regimes separately.

### 3.1. Subcritical regime ( $|\varepsilon_w| < |\varepsilon_w^{\text{cr}}|$ )

When there is no surface interaction ( $\varepsilon_w = 0$ ), the partition coefficient  $K$  is known to vary with the ratio  $2R_{g0}/D$ , but not individually. A plot of  $K$  vs.  $2R_{g0}/D$  for different chain sizes  $R_{g0}$  and slit widths  $D$  will collapse into a single master curve as confirmed earlier [42]. When the surface interaction is weak, such as  $\varepsilon_w = -0.1$ , such scaling plot still holds to a good degree. When  $\varepsilon_w = -0.2$ , one can clearly see the deviation from the master plot as shown in Fig. 2. The filled symbols in Fig. 2 are data for  $\varepsilon_w = 0.0$ , which is fitted to the scaling law dependence  $\beta\Delta\mu_{\text{conf}} \sim (2R_{g0}/D)^{1/\nu}$  where  $\nu = 0.58$  in our model. Data in Fig. 2 reveal that in the presence of attractive interaction, the smaller the slit width  $D$ , the more deviation of  $\beta\Delta\mu_{\text{conf}}$  from the master curve obtained when  $\varepsilon_w = 0.0$ . If one compares  $\beta\Delta\mu_{\text{conf}}$  at the same confinement strength,  $2R_{g0}/D$ , then  $\beta\Delta\mu_{\text{conf}}$  for short chains in the narrow slit is smaller than for the corresponding long chains in the wide slit but with same confinement strength.

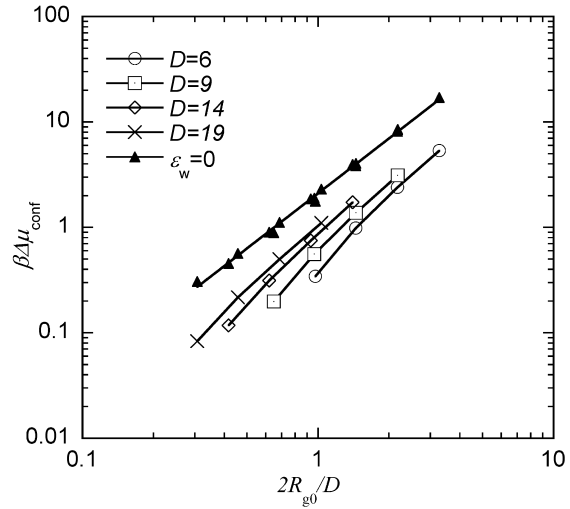


Fig. 2. The plot of confinement free energy  $\beta\Delta\mu_{\text{conf}}$  vs. confinement strength  $2R_{g0}/D$  of a single chain with  $N = 25, 50, 100,$  and  $200$  partitioning into a slit of different width in the subcritical regime. The filled symbols are data when  $\varepsilon_w = 0$  and the open symbols are data when  $\varepsilon_w = -0.2$ .

In order to find the universal relationship between  $K$  and  $N$  and  $D$  in the subcritical regime, we used the following scaling arguments. In the case of a long chain in narrow slit, the confined chain maybe viewed as being composed of blobs of size of slit width  $D$ . The confinement free energy per blob is  $k_B T$  when there is no surface interaction [27]. Therefore, one has  $\Delta\mu_{\text{conf}} = (N/g)k_B T = (R_{g0}/D)^{1/\nu}k_B T$  where  $g$  is the number of monomers in a blob of size  $D$ ,  $\nu$  is the Flory exponent. If there is a weak surface interaction, one may assume that the chain is still composed of blobs of size  $D$ . The confinement free energy can be broken into two parts, the enthalpic interaction due to the attractive interaction and the entropic due to the loss of configurational entropy.

$$\beta\Delta\mu_{\text{conf}} = \beta\Delta H - k_B \Delta S \quad (1)$$

The entropic free energy maybe assumed to be the same as that in the absence of the surface interactions since one still needs to confine the same number of blobs in the slit. The enthalpic interaction can be estimated. We assume that  $g$  monomers in a blob are distributed homogeneously in a sphere of radius  $D$ , and only the monomers in the top and the bottom crown of thickness  $a$  are in contact with the wall (note this assumption does not lead to a homogeneous density profile across the slit, see discussion in the later section). The crown volume is approximately given by  $a^2 D$  when  $a \ll D$ . Therefore, the number of monomers contacting with the wall per blob is given by  $g(a/D)^2$ . One obtains

$$\beta\Delta H \cong \left(\frac{N}{g}\right)g\left(\frac{a}{D}\right)^2 \varepsilon_w = N(a/D)^2 \varepsilon_w \quad (2)$$

Therefore, one may expect the free energy per chain in the

presence of the weak attractive interaction

$$\beta\Delta\mu_{\text{conf}} = c_1 N(a/D)^2 \varepsilon_w + c_2 (2R_{g0}/D)^{1/\nu} \quad (3)$$

where  $c_1$  and  $c_2$  are two unknown coefficients.

The above scaling results can be checked when one examines  $\Delta\Delta\mu$  that accounts for the enthalpic interaction

$$\Delta\Delta\mu = \Delta\mu(\varepsilon_w \neq 0) - \Delta\mu(\varepsilon_w = 0) = \Delta H \quad (4)$$

Fig. 3 presents the plot of  $\beta\Delta\Delta\mu/\varepsilon_w$  vs.  $N(a/D)^2$  for data with  $\varepsilon_w = -0.1$ . The scaling is observed reasonably except some small deviations when  $D = 19$ . The data in Fig. 3 is approximately linear. The same scaling plot is observed for  $\varepsilon_w$  up to the critical adsorption point. Note in Fig. 3,  $\varepsilon_w$  was fixed, but  $N$  and  $D$  were varied independently. Therefore, the scaling dependence of  $K$  on  $N$  and  $D$  in the first term of Eq. (3) is confirmed here, but not necessary the dependence on  $\varepsilon_w$ .

Cifra and Bleha [41] have also examined the variation of  $K$  for self-avoiding walk chains on the lattice at different surface interactions. They fitted their simulation data numerically and obtained the following empirical functional form

$$\beta\Delta\mu_{\text{conf}} = p(2R_{g0}/D)^q; \quad (5)$$

$$p = 2.04 + 2.01\varepsilon_w - 22.01\varepsilon_w^2; \quad q = 1.57 + 2.17\varepsilon_w$$

Their equation can be expanded in the power of  $\varepsilon_w$ ,  $\beta\Delta\mu_{\text{conf}} = (2.04) (2R_{g0}/D)^{1.57} + 6.43(2R_{g0}/D)^{1.57}\varepsilon_w + \dots$ . The first term in the expansion is the change of  $\beta\Delta\mu_{\text{conf}}$  in the non-adsorptive slit, that corresponds to our the second term, the entropic term in Eq. (3) (the numerical factors obtained are different in the two studies because they have studied primarily weak confinement limit). The second term gives the linear dependence on  $\varepsilon_w$ , which corresponds to our first term, the enthalpic term, in Eq. (3), however, the scaling dependence on  $N$  and  $D$  in the prefactor of  $\varepsilon_w$  is

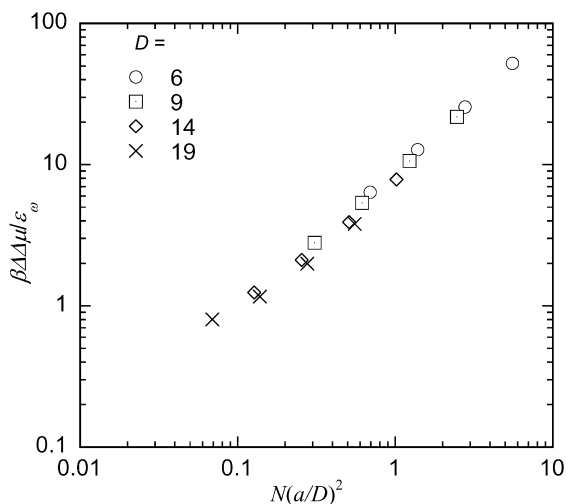


Fig. 3. The plot of  $\beta\Delta\Delta\mu/\varepsilon_w$  vs.  $N(a/D)^2$  where  $\Delta\Delta\mu = \Delta\mu_{\text{conf}}(\varepsilon_w = -0.1) - \Delta\mu_{\text{conf}}(\varepsilon_w = 0)$ . Data are for a single chain with different  $N$  partitioning into different slit width  $D$ . The surface interactions  $\varepsilon_w = -0.1$ .

totally different in the two equations. If their equation is correct, then a plot of  $\beta\Delta\mu_{\text{conf}}$  against  $2R_{g0}/D$  for a fixed  $\varepsilon_w$  in the subcritical regime should still form a master curve for different  $N$  and  $D$ . We have clearly shown in Fig. 2 that does not hold. Their equation is unlikely to be correct. These authors obtained their equation for a set of simulation data where  $N$  and  $D$  were not independently varied ( $N$  was held fixed while only  $D$  was varied).

According to our arguments that lead to Eq. (3),  $\beta\Delta\Delta\mu/\varepsilon_w$  would be a measure of the number of the contacts between the polymer beads and the surfaces of the slit and, therefore, one may compare this value at different surface interactions. Fig. 4 presents the overlap of data sets with  $\varepsilon_w = -0.1$  and  $-0.2$ . The number of contacts of the polymer with the surfaces at different surface interactions is close to each other, although it is not exactly the same. The number of contacts is slightly higher when  $\varepsilon_w$  becomes more attractive. This suggests the dependence of  $K$  on  $\varepsilon_w$ , expressed in Eq. (3) is good to a first degree of approximation. However, there might be higher order terms of  $\varepsilon_w$  that should be included in Eq. (3).

The density profiles in the confined slit also support the above scaling arguments. Our simulations are performed with a single chain in a lattice of  $250a \times 250a \times (D+1)a$  and the density profile  $\phi(z)$  is the percent of occupied sites in each layer. A normalization factor  $D/aN$  is needed,  $\phi_n(z) = \phi(z)D/aN$ , in order to compare the density profiles for different  $N$  and  $D$ . If the chain is composed of blobs of size of slit width  $D$ , then the normalized density profiles,  $\phi_n(z)$ , for different chain lengths in the same slit are the same. Note when one assumes that monomers in a blob are distributed homogeneously in a sphere of blob size, this does not lead to a flat density profile across the slit. There are more monomers from the center slice of the sphere than from the edge, hence high density in the center layers. Density profiles in different slit widths are also the same

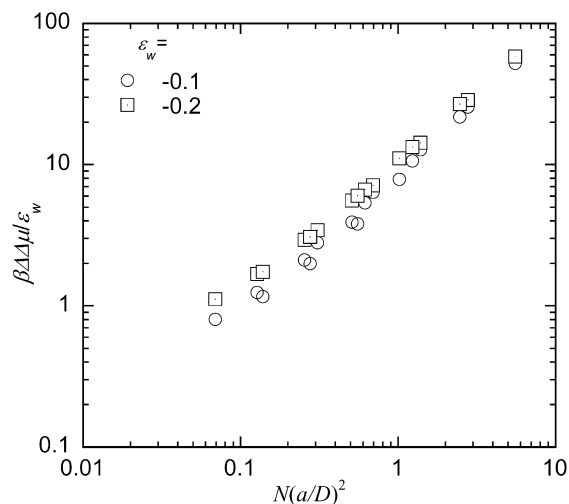


Fig. 4. The plot of  $\beta\Delta\Delta\mu/\varepsilon_w$  vs.  $N(a/D)^2$  in the subcritical regime with two surface interactions,  $\varepsilon_w = -0.1$  and  $-0.2$ . Each set of data contain results obtained with different  $N$  and different  $D$ .

when the  $z$  coordinate is normalized by slit width  $D$ . Fig. 5 confirms the scaling prediction where representative density profiles for different chain lengths  $N$  and different slit widths  $D$  are presented for  $\varepsilon_w = 0$ . The density profiles fit into a universal curve. Such universal density profiles do not apply if the size of the chains is smaller than the slit width. As a result, we have identified three systems,  $N = 25$  and  $50$  in  $D = 19$  and  $N = 25$  in  $D = 14$ , that do not satisfy the condition  $R_{g0} < D$ . Gorbunov and Skvortsov have predicted that the universal density profile for the ideal chain in narrow slit is given by  $\sin^2(z\pi/D)$ . Using our scaling arguments, we could derive an expected density profile but the form is very cumbersome. Instead, we fitted our universal density profile for self-avoiding chains to  $\sin^p(z\pi/D)$  with  $p = 1.3-1.4$ . When  $\varepsilon_w \neq 0$  and in the subcritical regime, a universal density profile is still obtained for different  $N$  and  $D$ , but the profile is flattened. The density near the wall is higher and the peak is lowered when  $\varepsilon_w \neq 0$ .

The density at the first layer near the surfaces  $\phi(a)$  accounts for the number of surface contacts. Since  $\phi_n(z) = \sin^p(z\pi/D)$ , we obtain  $\phi(a) \sim N/(a/D)^{p+1}$ , whereas the scaling arguments using the blob concepts give  $\phi(a) \sim N/(a/D)^2$ . The data in Figs. 3 with  $\varepsilon_w = -0.1$  actually gives a better scaling plot using  $\beta\Delta\Delta\mu/\varepsilon_w$  vs.  $N(a/D)^{p+1}$  with  $p = 1.3$ . However, data set with  $\varepsilon_w = -0.2$  give somewhat worse scaling plots using  $N(a/D)^{p+1}$ .

Fig. 6 presents the comparison of the radius gyration of the confined chains in the absence (open symbols) and presence of (filled symbols) surface interactions ( $\beta\varepsilon_w = -0.2$ ). The Y-axis is  $R_{gxy}^{\text{conf}}/R_{gxy}^0$  (data points above  $y = 1$ ) and  $R_{gz}^{\text{conf}}/R_{gz}^0$  (data points below  $y = 1$ ) where  $R_{gxy}$  and  $R_{gz}$  are the radius of gyration in the  $xy$  and  $z$  directions, and superscript ‘conf’ and ‘0’ stand for confined chain and unconfined chain, respectively. Data for different chain

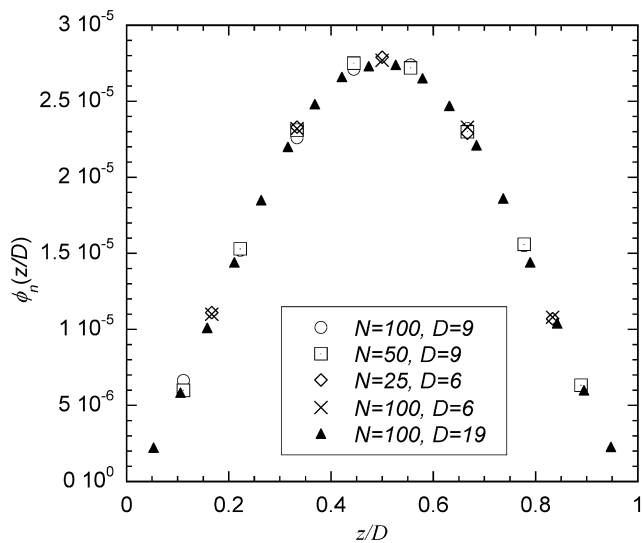


Fig. 5. The plot of normalized density profiles  $\phi_n(z) = \phi(z)Na/D$  vs. the normalized coordinate  $z/D$  for a single chain of different lengths  $N$  in different slit widths  $D$  when the surface/wall interaction  $\varepsilon_w = 0$ .

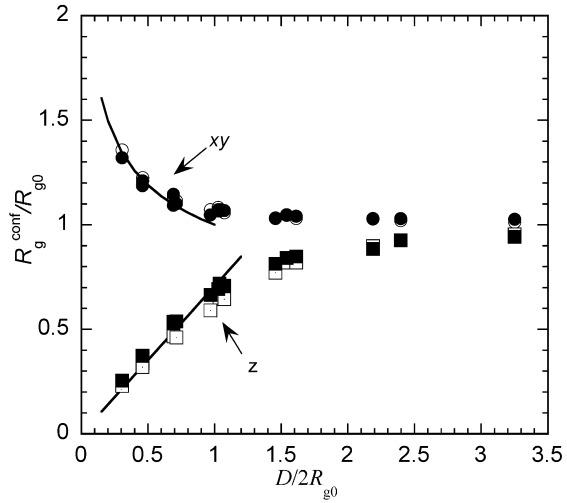


Fig. 6. The comparison of the radius of gyration of the confined chain,  $R_g^{\text{conf}}/R_{g0}$  when  $\varepsilon_w = 0$  (the filled symbols) with that when  $\varepsilon_w = -0.2$  (open symbols) in the subcritical regime. The filled symbols are data when  $\varepsilon_w = 0$  and the open symbols are data when  $\varepsilon_w = -0.2$ . The Y-axis is  $R_{gxy}^{\text{conf}}/R_{gxy}^0$  and  $R_{gz}^{\text{conf}}/R_{gz}^0$  where ‘0’ stands for the value of the unconfined chain. The two solid lines are the fit to the scaling predictions  $R_{gxy}^{\text{conf}}/R_{gxy}^0 \sim (D/2R_{g0})^{1/4}$ , and  $R_{gz}^{\text{conf}}/R_{gz}^0 \sim D$  at strong confinement.

length  $N$  and slit width  $D$  form master curves for the  $xy$  and  $z$  components, respectively, when plotted in this way. Note there are hardly any differences between the data set with  $\varepsilon_w = 0$  and data set with  $\varepsilon_w \neq 0$ , except some small difference in the  $z$ -component. Weakly attractive surface interaction does not perturb the conformation of the chain in the slit significantly. This is true up to  $\varepsilon_w = -0.3$ . The variation of the shape of the chain upon increase of the confinement strength is well understood in non-adsorptive slit [42]. The chain first re-orient itself so its long axis is parallel to the walls and then at strong confinement ( $D/2R_{g0} < 1$ ) the chain is deformed. The data in Fig. 6 at strong confinement conforms to the scaling predictions, which is drawn by the solid lines. The  $z$ -component is proportional to the slit width  $D$ ,  $R_{gz}^{\text{conf}}/R_{gz}^0 \sim D/2R_{g0}$ , and the  $xy$ -component is given by  $R_{gxy}^{\text{conf}}/R_{g0} \sim (D/2R_{g0})^{1/4}$ .

Therefore, one can summarize that in the subcritical regime, the conformation of the chain is largely controlled by confinement. The weak interaction between the surfaces of the pore with the chain does not significantly modify the chain conformation, but lowers the free energy of the chain through the surface contacts. In the case of a long chain in a narrow slit, the chain can be viewed as connected sequences of blobs of size  $D$ . The free energy of the chain inside the blob is given approximately by Eq. (3), where the second entropy term is greater than the first enthalpy interaction.

### 3.2. Adsorptive regime ( $|\varepsilon_w| > |\varepsilon_w^{\text{cr}}|$ )

In the adsorptive regime, the free energy of a chain inside the slit is lower than that of a chain outside of the slit because of the attractive enthalpy interaction between the chain and the slit surface. The partition coefficient  $K$  as a



result is greater than one. The confinement free energy  $\beta\Delta\mu_{\text{conf}}$  may still be separated to two parts: the enthalpic and the entropic parts. However, the enthalpic interaction dominates the partitioning and is larger than the entropic interaction in the adsorptive regime.

In the adsorptive regime, the trend of dependence of the partition coefficient on the surface interactions is the same as in the subcritical regime. The stronger the surface interaction, the larger the partition coefficient. The dependences of the partition coefficient on the chain length and slit width are reversed from that in the subcritical regime. The longer the chain, the more extensive contacts the chain will make with the slit surfaces and, therefore, the larger the partition coefficient. A narrower slit on the other hand would also give rise to more contacts with the chain and lead to a larger partition coefficient. These effects are seen in Fig. 7, which presents the plot of  $\beta\Delta\mu_{\text{conf}}$  for a single chain as a function of chain length confined in a slit of different width at  $\varepsilon_w = -0.4$ . One can see that  $\beta\Delta\mu_{\text{conf}}$  is more negative (larger partition coefficient) for longer chains and narrower slits, a different trend from that in the subcritical regime. These are all because the enthalpic term is dominating in the adsorptive regime.

In the adsorptive regime, a chain can be adsorbed on a single standing solid surface and form an adsorbed layer. The mean-field theory [35] and the scaling theory [27] predict that the thickness of the adsorbed layer above a single standing surface is given by  $h = a\Delta^{-3/2}$  where  $\Delta = |1 - \varepsilon/\varepsilon_c|$ . When the chain is in the slit with adsorptive surfaces, one may have two different regimes depending on the relative values of  $h$  and  $D$ :  $h > D$  and  $h < D$ . When  $h < D$ , the chain in the slit will be adsorbed on either side of the surfaces of the slit. In this case, one may expect that the free energy of the chain inside the slit have little dependence on the slit width  $D$ . When  $h > D$ , the adsorbed layer will be disturbed and

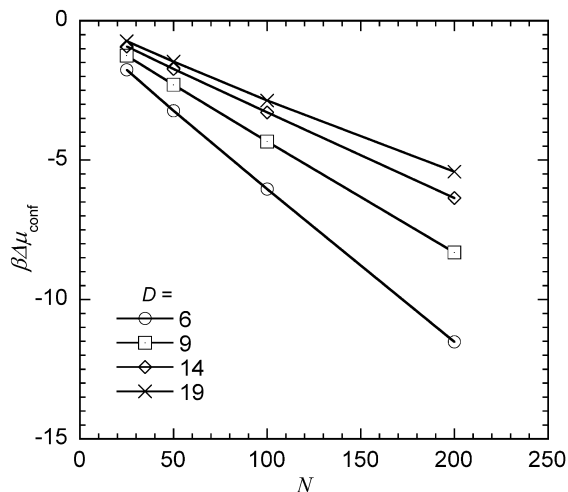


Fig. 7. The plot of the confinement free energy  $\beta\Delta\mu_{\text{conf}}$  in the adsorptive regime ( $\varepsilon_w = -0.4$ ) as a function of chain length  $N$  in different slit widths  $D$ .

the thickness will be controlled by the slit width  $D$ . In this case, one may attempt to assume that the blob size is still  $D$ , then the number of monomers in contacting with the wall is still given by Eq. (3). However, we find that this is not true. The plot  $\Delta\Delta\mu/\varepsilon_w$  vs.  $N(a/D)^2$  for data with different  $D$  does not yield a common curve (figure not shown). The data for larger  $D$  shifted upward, implying that the chain has more contacts with the surface of the slit than predicted according to the scaling  $N(a/D)^2$ .

The density profiles in the slit reveal the difference between the adsorptive regime and the subcritical regime. In wide slit with strong adsorptive interaction where  $h < D$ , we find that it is somewhat difficult to obtain the symmetric density profiles. The chain may be adsorbed on either side, which gives rise to an unsymmetric density profile. One has to allow for long equilibration times between snapshots to obtain a good density profile. The density profiles obtained, however, are all same for different  $N$  in wide slits in contrast to the chains in wide slit in non-adsorptive regime. Density profiles in narrow slits for different  $N$  are also the same since now the characteristic length scale is the slit width  $D$  and is independent of the chain length. However, normalized density profiles in different slit width are no longer the same, as shown in Fig. 8 for a chain with  $N = 200$  in different slit widths at  $\varepsilon_w = -0.4$ . One may identify that  $h > D$  for these systems. The density in the middle of the slit is higher in the narrow slit than in the wide slit. Clearly the blob picture must be modified to account for the observation seen in the adsorptive regime. The number of surface contact with the wall cannot be the same as in the subcritical regime.

Instead, we find that it may scale with  $N(a/D)$  in the adsorptive regime. Fig. 9 presents the plot of  $\beta\Delta\Delta\mu/\varepsilon_w$  vs.  $N(a/D)$  when  $\varepsilon_w = -0.4$ . A good scaling fit is obtained at  $\varepsilon_w = -0.4$ . At  $\varepsilon_w = -0.5$ , the scaling plot holds for data in  $D = 6, 9$ , and  $14$ , but not for data set with  $D = 19$ . This implies that when  $h > D$ , the free energy of a single chain in

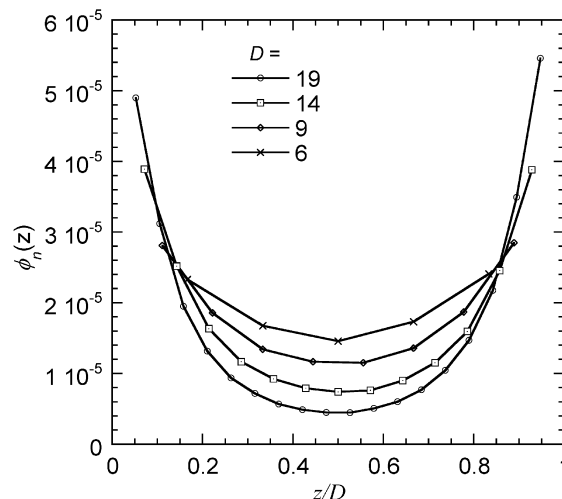


Fig. 8. The normalized density profiles of a single chain of  $N = 200$  in different slit widths  $D$  in the adsorptive regime at  $\varepsilon_w = -0.4$ .

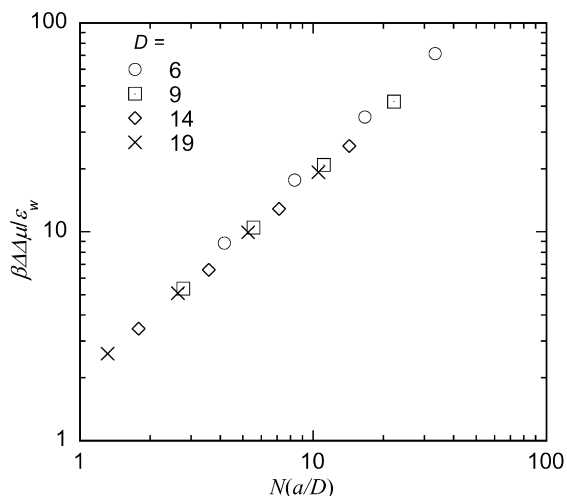


Fig. 9. The plot of  $\beta\Delta\Delta\mu/\varepsilon_w$  vs.  $N(a/D)$  in the adsorptive regime when  $\varepsilon_w = -0.4$ , where  $\Delta\Delta\mu = \Delta\mu_{\text{conf}}(\varepsilon_w \neq 0) - \Delta\mu_{\text{conf}}(\varepsilon_w = 0)$ .

the adsorptive slit is given by

$$\beta\Delta\mu_{\text{conf}} = c_1 N(a/D)\varepsilon_w + c_2 (2R_{g0}/D)^{1/\nu} \quad (6)$$

This result, however, is not unfamiliar. The free energy of a single chain adsorbed on a single standing solid surface according to the mean-field theory is given by the above equation except the slit width  $D$  is replaced by the thickness of adsorbed layer [27]. The thickness of the adsorbed layer on a single standing solid surface is adjustable which can be obtained by minimizing the above expression. When the chain is confined in a slit with adsorptive walls, the thickness of the adsorbed layer is no longer adjustable if  $h > D$  and the thickness of the adsorbed layer is given by  $D$  instead. Then Eq. (6) holds. It is not surprising that our data fit into Eq. (6). We have examined here  $\varepsilon_w = -0.4$  and  $-0.5$ , which are slightly above the critical adsorption point. When  $\varepsilon_w$  is only slightly above the critical adsorption point, the thickness of the adsorbed layer is about the size of the chain,  $R_{g0}$ . Therefore, most of our data at  $\varepsilon_w = -0.4$  would fall in the regime that  $h > D$ . Data set in  $D = 19$  with  $\varepsilon_w = -0.5$  did not fit into Eq. (6) because in this case  $h < D$ .

Therefore, in the adsorptive regime and  $h > D$ , the free energy of the chain inside the slit is given by Eq. (6). Although expression like Eq. (6) is often given, it is not apparent that Eq. (6) should hold for a chain in the adsorptive slit. We also note that the scaling theory using blob concepts do not readily lead to Eq. (6). Other correct arguments are needed to account for the validness of Eq. (6).

One can now see that the enthalpic term of the confinement free energy maybe written as  $N(a/D)^x \varepsilon_w$  with  $x$  varies from 2.0 or larger in the subcritical regime to 1.0 in the adsorptive regime. Note the entropic term in Eq. (3) or Eq. (6) can be re-expressed as  $N(a/D)^{1/\nu}$ , and the enthalpic term and the entropic terms are of opposite sign. Therefore, one may expect that the crossover from the subcritical regime to the adsorptive regime at the critical adsorption point occur when the exponent in the first term is exactly

$1/\nu$ . This then would lead to a critical behavior that the partition coefficient would be independent of  $N$  and  $D$ . This is indeed confirmed in our simulation data. Data set at  $\varepsilon_w = -0.276$  can be best collapsed into a single master curve when  $\beta\Delta\Delta\mu$  is plotted against  $N(a/D)^{1/\nu}$ , not against  $N(a/D)^{2.0}$  or  $N(a/D)^{1.0}$ . However, the two terms given here are only the dominant terms. There are other higher order terms that may become important at the critical adsorption point and lead to a weak dependence of  $K$  on  $N$  and  $D$  even at the critical adsorption point as observed earlier [41].

Finally, we present the radius of gyration of the chain in the adsorptive regime in different slit width in Fig. 10. The solid symbols are data when  $\varepsilon_w = 0$ . The open symbols are data for  $\varepsilon_w = -0.5$  and different symbols are used for different slit width. In wide slit, one observes the expansion of the  $xy$ -component and the reduction of the  $z$ -component compared to the same chain in non-adsorptive regime. In narrow slits at strong confinement, the  $z$ -component is slightly higher than in non-adsorptive regime. This is due to the difference in the monomer distributions in the two regimes. In the adsorptive regime, more monomers are distributed on the two surfaces, whereas in the non-adsorptive regime, more monomers are in the center of slit. Therefore, the measured radius of gyration of the chain in the  $z$ -component is slightly larger than that in the non-adsorptive regime as a result of the difference in the monomer distributions in the slit.

The variation of the radius of gyration in the  $xy$  and  $z$  components as the slit width  $D$  decreases for a given chain length is also different from that in the non-adsorptive regime. In the non-adsorptive regime, the  $xy$ -component will continually increase and the  $z$ -component will continually decrease as the slit width  $D$  decreases. In the adsorptive regime, one can observe a reversed behavior at

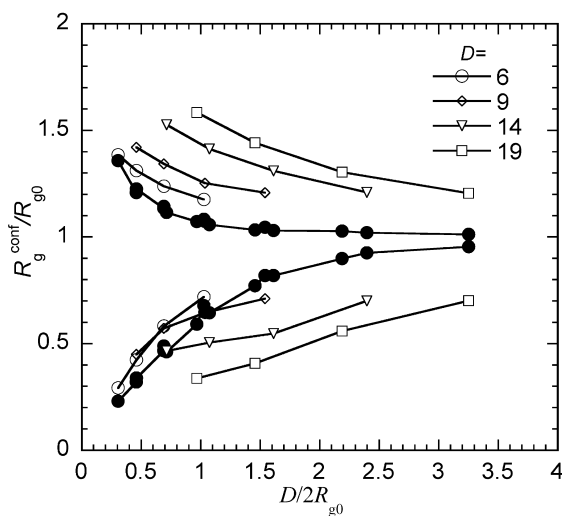


Fig. 10. The comparison of the radius of gyration of the confined chain,  $R_g^{\text{conf}}/R_{g0}$  when  $\varepsilon_w = 0$  (the filled symbols) with that when  $\varepsilon_w = -0.5$  (open symbols) in the adsorptive regime. The Y-axis is  $R_{xy}^{\text{conf}}/R_{xy}^0$  and  $R_{gz}^{\text{conf}}/R_{gz}^0$  where '0' stands for the value of the unconfined chain. Data for  $\varepsilon_w = -0.5$  in different slit widths  $D$  are shown in different symbols.

strong adsorption. The  $xy$ -component can decrease and the  $z$ -component can increase as the slit width  $D$  decreases. When the slit is wide, the chain is adsorbed on either side of the surface and the conformation of the chain is severely deformed in order to have maximum surface contacts. When the slit gets narrower, the chain can be adsorbed on both sides of the slit surfaces. Therefore, the chain can achieve maximum surface contacts yet adopt a less severely deformed conformation. The chain is, therefore, less flattened, giving rise to a decrease in the  $xy$ -component and an increase in the  $z$ -component.

#### 4. Conclusions

We have considered the partitioning of a single polymer chain into a slit with attractive surface interaction in an athermal solvent through Monte Carlo simulations. Two regimes have been studied, the subcritical regime and the adsorptive regime in narrow slits. The free energy of the chain in the pore is separated to two terms, the enthalpic term arising from the surface interaction and the entropic term of confining the chain inside the slit. Since, we are considering a long chain in narrow slit, the entropic confinement term is replaced by the confinement free energy of the same chain in the pore with no surface interaction,  $\Delta\mu(\varepsilon_w = 0)$ , which is given by  $(R_{g0}/D)^{1/\nu}$ . The enthalpic term is given by  $N(a/D)^x\varepsilon_w$  with  $x \sim 2.0$  or larger in the subcritical regime and  $\sim 1.0$  in the adsorptive regime. We gave a scaling argument based on blob concepts that would lead to an exponent  $x = 2.0$  for a long chain in narrow slit in the subcritical regime. The density profiles in the subcritical regime also support such blob concepts. In the adsorptive regime, however, we do not have a valid argument that could support the observed exponent  $x \sim 1.0$ . The density profiles obtained in the adsorbed regime were non-universal unlike in the non-adsorptive slit. At the critical adsorption point,  $x = 1/\nu$  is observed, which could then explain the critical behavior where  $K$  has little dependence on  $N$  or  $D$ .

In this study, the scaling dependence of  $K$  on  $N$  and  $D$  are confirmed in different regimes, but the scaling dependence on  $\varepsilon_w$  is not confirmed. We consider the scaling dependence on  $\varepsilon_w$  is of less importance because in real situations one cannot vary  $\varepsilon_w$  at will. One is likely working at a fixed  $\varepsilon_w$  in certain regime and would be interested in the scaling dependence of  $K$  on  $N$  and  $D$ . Our data also include only the dominant term of surface interactions. There may be higher order terms of  $\varepsilon_w$  that should be included in Eqs. (3) and (6). Moreover, Eqs. (3) and (6) are only applicable for long chains in narrow slit and  $h > D$  if in adsorptive regime. Also the exponent in the enthalpic term  $N(a/D)^x\varepsilon_w$  should be considered as a variable changing from their respective values in different regime.

#### Acknowledgements

This research is supported by the National Science Foundation (DMR-9876360) and the Petroleum Research Fund (PRF-32707-GB5) administered by the American Chemical Society. We also acknowledge the computer resource support provided by the North Carolina Super Computer Center.

#### References

- [1] Casassa EF. *J Polym Sci, Polym Lett Ed* 1967;5:773.
- [2] Casassa EF, Tagami Y. *Macromolecules* 1969;2:14.
- [3] Colton CK, Satterfield CN, Lai CJ. *AICHE-J* 1975;21:289.
- [4] Daoud M, de Gennes PG. *J Phys (Paris)* 1977;38:85.
- [5] Daoudi S, Brochard F. *Macromolecules* 1978;11:751.
- [6] Satterfield CN, Colton CK, de Turckheim B, Copeland T. *AICHE-J* 1978;24:939.
- [7] de Gennes PG. *Scaling concepts in polymer physics*. Ithaca: Cornell University Press; 1979.
- [8] Davidson MG, Suter UW, Deen WM. *Macromolecules* 1987;20:1141.
- [9] Giddings JC. *Unified separation science*. New York: Wiley; 1991.
- [10] Teraoka I. *Prog Polym Sci* 1996;21:89.
- [11] Cifra P, Bleha T, Romanov A. *Makromol Chem, Rapid Commun* 1988;9:355.
- [12] Bleha T, Cifra P, Karasz FE. *Polymer* 1990;31:1321.
- [13] Yethiraj A, Hall CK. *Macromolecules* 1990;23:1865.
- [14] Honeycutt JD, Thirumalai D. *J Chem Phys* 1990;90:4542.
- [15] Yethiraj A, Hall CK. *Mol Phys* 1991;73:503.
- [16] Kierlik E, Rosinberg EL. *J Chem Phys* 1994;100:1716.
- [17] Thompson AP, Glandt ED. *Macromolecules* 1996;29:4314.
- [18] Wang Y, Teraoka I. *Macromolecules* 1997;30:8473.
- [19] Cifra P, Bleha T, Wang Y, Teraoka I. *J Chem Phys* 2000;113:8313.
- [20] Wang Y, Cifra P, Teraoka I. *Macromolecules* 2001;34:127.
- [21] Pasch H, Trathnigg B. *HPLC of polymers*. Berlin: Springer; 1990.
- [22] Pasch H, Brinkmann C, Much H, Just U. *J Chromatogr* 1992;623:315.
- [23] Berek D, Jančo M, Meira GR. *J Polym Sci A* 1998;36:363.
- [24] Jančo M, Hirano T, Kitayama T, Hatada K, Berek D. *Macromolecules* 2000;33:1710.
- [25] Falkenhagen J, Much H, Stauff W, Müller AHE. *Macromolecules* 2000;33:3687.
- [26] Lee W, Lee H, Lee HC, Cho D, Chang T, Gorbunov AA, Roovers J. *Macromolecules* 2002;35:529.
- [27] de Gennes PG. *Macromolecules* 1981;14:1637.
- [28] de Gennes PG. *Macromolecules* 1982;15:492.
- [29] Simha R, Frisch HL, Eirich FR. *J Chem Phys* 1953;57:584.
- [30] Frisch HL, Simha R. *J Chem Phys* 1956;24:652.
- [31] Silberbger A. *J Phys Chem* 1962;66:1872. see also p. 1884.
- [32] DiMarzio EA. *J Chem Phys* 1965;42:2101.
- [33] (a) Roe RJ. *J Chem Phys* 1965;43:1591. (b) Roe RJ. *J Chem Phys* 1966;44:4264.
- [34] (a) Scheutjens JM, Flerer GJ. *J Phys Chem* 1979;83:1619. (b) Scheutjens JM, Flerer GJ. *J Phys Chem* 1980;84:178.
- [35] Flerer GJ, Cohen Stuart MA, Scheutjens JM, Cosgrove T. *Polymers at interfaces*. London, UK: Chapman & Hall; 1993.
- [36] Gorbunov AA, Skvortsov A. *Adv Colloid Interface Sci* 1995;62:31.
- [37] Milchev A, Wolfgang P, Binder K. *Macromol Theory Simul* 1994;3:305.
- [38] Pandey R, Milchev A, Binder K. *Macromolecules* 1997;30:1194.
- [39] Milchev A, Binder K. *Macromolecules* 1996;29:343.
- [40] Cifra P, Bleha T. *Macromolecules* 2001;34:605.
- [41] Gong Y, Wang Y. *Macromolecules* 2002;35:7492.
- [42] Wang Y, Teraoka I. *Macromolecules* 2000;33:3478.